Photoaffinity Labeling of Mutant Neurokinin-1 Receptors Reveals Additional Structural Features of the Substance P/NK-1 Receptor Complex†

Douglas Macdonald,[‡,§] Dale F. Mierke,[||,⊥] Hanzhong Li,[‡] Maria Pellegrini,[||] Bruce Sachais,[#] James E. Krause,[▽] Susan E. Leeman,[‡] and Norman D. Boyd*[,‡]

Department of Pharmacology and Experimental Therapeutics, Boston University School of Medicine, Boston, Massachusetts 02118, Department of Molecular Pharmacology, Division of Biology and Medicine, and Department of Chemistry, Brown University, Providence, Rhode Island 02912, Department of Pathology and Laboratory Medicine, University of Pennsylvania, Philadelphia, Pennsylvania 19104, and Neurogen Corporation, Branford, Connecticut 06405

Received August 9, 2000; Revised Manuscript Received December 19, 2000

ABSTRACT: Photoaffinity labeling, receptor site-directed mutagenesis, and high-resolution NMR spectroscopy have been combined to further define the molecular details of the binding of substance P (SP) to the rat neurokinin-1 (NK-1) receptor. Mutant NK-1 receptors were constructed by substituting Ala for Met174 and/or Met181: residues previously identified as the sites of covalent attachment of radioiodinated, photoreactive derivatives of SP containing *p*-benzoyl-L-phenylalanine (Bpa) in positions 4 and 8, respectively. Photoaffinity labeling of the M181A mutant using radioiodinated Bpa[8]-SP resulted in a marked reduction in photoincorporation efficiency compared to the wild-type receptor. In contrast, photoaffinity labeling of the M174A mutant using radioiodinated Bpa[4]-SP gave the unexpected result of an increase in the efficiency of photoincorporation compared to the wild-type receptor. Enzymatic and chemical fragmentation analysis of the photolabeled receptor mutants established that the sites of covalent attachment were not the substituted alanine, but rather the other methionine on the second extracellular (E2) loop sequence, that is not the primary site of attachment in the wild-type receptor. The results thus suggest a close spatial relationship between Met174 and Met181 on the NK-1 receptor. To evaluate this structural disposition, NMR analyses were performed on a synthetic peptide with a sequence corresponding to the entire E2 loop and segments of the adjoining transmembrane helices to anchor the peptide in the lipids used to mimic a membrane. The structural features of the E2 loop include a centrally located α-helix, extending from Pro175 to Glu183, as well as smaller α-helices at the termini, corresponding to the transmembrane regions. The two methionine residues are located on the same face of the central α-helix, approximately 11 Å apart from each other, and are therefore consistent with the conclusions of the photoaffinity labeling results.

The multiple physiological actions of the peptide substance P (SP),[1] including the transmission of pain, neurogenic inflammation, and a spectrum of behavioral responses, are mediated via the binding of SP to the neurokinin-1 (NK-1) receptor (SP receptor), a member of the G protein-coupled receptor (GPCR) superfamily of heptahelical transmembrane signaling proteins (*1*). Detailed structural studies of receptor proteins have led to significant advances in our understanding of how structure renders physiological and pharmacological function. The determination of the structure of ligand−receptor complexes, here substance P and the NK-1 receptor, is an important step in the understanding of the molecular basis of peptide ligand recognition and receptor activation.

The introduction of the photoactivatable amino acid *p*-benzoyl-L-phenylalanine (Bpa) for the synthesis of highly efficient photoactivatable peptide probes (*2*) has led us to develop a Bpa scanning approach for analysis of SP/NK-1 receptor interactions. We first reported the use of *p*-benzoyl-L-phenylalanine[8]-SP (Bpa[8]-SP), where Phe[8] was substituted by Bpa to make a specific, high-affinity, peptide probe for the NK-1 receptor (*3*). This ligand was radioiodinated using Bolton−Hunter conjugation to Lys[3], producing ^{125}I(BH)Bpa[8]-SP. Receptor fragmentation analysis and MALDI mass spectrometry of an isolated fragment identified the site of covalent attachment of the benzophenone carbonyl in ^{125}I(BH)Bpa[8]-SP as the terminal methyl group of Met181 in the second extracellular (E2) loop of the rat NK-1 receptor (*4*). A second SP photoligand developed in our laboratory replaced Pro[4] in the SP peptide with Bpa. Similar method-

† This work was supported in part by grants from the National Institutes of Health, NS-31346 (N.D.B.) and R29-GM54082 (D.F.M.).

* To whom correspondence should be addressed at the Department of Pharmacology and Experimental Therapeutics, Room L611, Boston University School of Medicine, 80 E. Concord St., Boston, MA 02118. Tel.: (617)638-4387; Fax: (617)638-4329; E-mail: nboyd@bu.edu.

‡ Department of Pharmacology and Experimental Therapeutics, Boston University School of Medicine.

§ Current address: CNS Biochemical Pharmacology, Aventis Pharmaceuticals Inc., Bridgewater, NJ 08807.

|| Department of Molecular Pharmacology, Brown University.

⊥ Department of Chemistry, Brown University.

Department of Pathology and Laboratory Medicine, University of Pennsylvania.

▽ Neurogen Corp.

10.1021/bi001880x CCC: $20.00
Published on Web 02/02/2001

ologies were applied to the ^{125}I(BH)Bpa^4-SP-photolabeled NK-1 receptor, and the covalent attachment site for this ligand was found to be Met174 also on the E2 loop (*5*).

The structural relationship between these two attachment sites on the NK-1 receptor has been difficult to assess. To extend our understanding of the role of these two methionine residues in peptide binding, we have undertaken two different, yet very complementary approaches: site-directed mutagenesis to replace Met174 and/or Met181 and high-resolution NMR studies of the regions of the receptor identified by photoaffinity labeling. The value of combining these methods has recently been demonstrated for the parathyroid hormone receptor to further define the ligand binding domain (*6, 7*).

Here we report the results from studies using both photoprobes, Bpa^4-SP and Bpa^8-SP, on receptor mutants in which Ala had been substituted for either Met174 or Met181. Additionally, the structural features of the E2 loop containing both of these residues have been determined by high-resolution NMR in order to investigate their spatial relationship. These results taken together with the photoaffinity results provide important insights into the interactions between SP and the NK-1 receptor.

EXPERIMENTAL PROCEDURES

Construction and Transfection of M174A, M181A, and M174A/M181A Mutant NK-1 Receptors. Site-directed mutagenesis was performed as previously described (*8*) using the M13-based oligonucleotide-directed in vitro mutagenesis system from Amersham. The nucleotide sequence of all mutated cDNAs used was verified by the chain termination method of Sanger (*9*) using the PRISM T7 Terminator Single-Stranded DNA Sequence Kit (Applied Biosystems, Foster City, CA), and sequences were analyzed on an automated 373A DNA Sequencer (Applied Biosystems). Mutant NK-1 receptor cDNAs were isolated from M13mp19 replicative form using *Hin*dIII and *Bam*HI restriction sites, and subcloned into pBS. The cDNAs were then subcloned into pM2-AH (*8*) using *Xho*I and *Bam*HI restriction sites. Plasmid DNA was purified using an anion exchange procedure (QIAGEN Inc.). Stable transfection of Chinese hamster ovary (CHO) cells was performed using 20 μg of DNA and a calcium phosphate procedure as previously described (*10*). These cells were grown and maintained in α-modified essential medium (Sigma) containing 10% fetal bovine serum (Life Technologies) and 800 μg/μL Geneticin (G418) (Gibco-BRL).

Equilibrium Displacement Binding Assays. Wild-type or mutant NK-1 receptor transfected CHO cells were harvested with Enzyme Free Cell Dissociation Buffer (Specialty Media, Lavellette, NJ), pelleted by centrifugation at 100*g* for 10 min, and resuspended in HEPES buffer (20 mM HEPES, 1 mM $CaCl_2$, 2.2 mM $MgCl_2$, 5 mM KCl, 120 mM NaCl, pH 7.4) supplemented with 6 mg/mL glucose and 0.6 mg/mL BSA. [^{125}I]Bolton−Hunter-conjugated SP [^{125}I(BH)-SP] was made as previously described (*3*), added to this resuspenstion, and incubated for 2 h in the presence of increasing concentrations of nonradiolabeled SP, Bpa^4-SP, Bpa^8-SP, ^{127}I(BH)Bpa^4-SP, or ^{127}I(BH)Bpa^8-SP [^{127}I derivatives were made as previously described (*4, 11*)]. After incubation, the cells were filtered through 0.1% polyethylenimine-treated Whatman GF/C filter paper and washed 3 times in 4 °C HEPES, pH 7.4, with a Brandel Harvester apparatus (Gaithersburg, MD), and the radioactivity was quantified by γ-spectrometry. These experiments were performed in duplicate and repeated at least 3 times.

Photoaffinity Labeling of Transfected Cells. Transfected CHO cells were harvested and resuspended in HEPES buffer, pH 7.4, supplemented with 6 mg/mL glucose and 0.6 mg/mL BSA, as described above. ^{125}I(BH)Bpa^4-SP or ^{125}I(BH)-Bpa^8-SP were made as previously described (*3, 5*) and added to the cell resuspension to give a final concentration of 1−2 nM. After a 2 h incubation in the dark at 4 °C with gentle agitation, the mixture was transferred to a 100 mm Petri dish, diluted 1:1 with ice-cold HEPES buffer, pH 7.4, and irradiated for 20 min on ice at a distance of 6 cm from a 100 W longwave (365 nm) UV lamp. Photolabeled cells were obtained through centrifugation, resuspended in Tris/EDTA buffer (5 mM Tris-HCl, 1 mM EDTA, pH 7.4) containing 0.1 mM phenylmethylsulfonyl fluoride, and sonicated 2 × 10 s with a Sonicator Cell Disrupter (Heat Systems−Ultrasonics, Inc.). Membranes were then obtained by centrifugation at 30000*g* for 1 h. The final pellet was resuspended in Tris/EDTA buffer and frozen at −20 °C.

Quantitative analysis of ^{125}I(BH)Bpa^4-SP and ^{125}I(BH)-Bpa^8-SP photoincorporation into wild-type, M174A, M181A, and M174A/M181A NK-1 receptors was performed as previously described (*3*). Briefly, the amount of photoligand incorporated into the receptors after photolabeling was determined by SDS−PAGE, autoradiography, and analysis of the radiolabeled 80 kDa receptor band. This was compared to the amount of photoligand specifically bound to the receptor before UV irradiation, determined by equilibrium filtration binding assay. Determination of the percent photoincorporation was performed at least 3 times, in duplicate.

Enzymatic and Chemical Fragmentation Analysis. Membrane preparations of photolabeled NK-1 receptors were thawed, solubilized in 50 mM Tris-HCl, pH 8.0, 1 mM $CaCl_2$ with 0.1% SDS (final concentration), and digested with increasing concentrations of trypsin, for 2 h at room temperature. After incubation, N^{α}-*p*-tosyl-L-lysine chloromethyl ketone (34 mg/mL DMSO) was added to the reaction in a 1:1000 dilution, and the mixture was heated for 10 min at 55 °C to terminate enzymatic activity.

Staphylococcus aureus V8 protease (V8) subcleavage was performed on SDS−PAGE-resolved and eluted tryptic receptor fragments. Passive elution of the tryptic fragments was performed by incubation of the excised gel piece in 100 mM NH_4HCO_3, 0.1% SDS at pH 7.8. The eluate was concentrated

[1] Abbreviations: ^{125}I(BH)-SP, (^{125}I-labeled Bolton−Hunter conjugate)Lys^3 substance P; ^{125}I(BH)Bpa^4-SP, (^{125}I-labeled Bolton−Hunter conjugate)Lys^3-*p*-benzoyl-L-phenylalanine^4 substance P; ^{125}I(BH)Bpa^8-SP, (^{125}I-labeled Bolton−Hunter conjugate)Lys^3-*p*-benzoyl-L-phenylalanine^8 substance P; Bpa, *p*-benzoyl-L-phenylalanine; Bpa^4-SP, *p*-benzoyl-L-phenylalanine^4 substance P; Bpa^8-SP, *p*-benzoyl-L-phenylalanine^8 substance P; CHO cells, Chinese hamster ovary cells; CNBr, cyanogen bromide; DMSO, dimethyl sulfoxide; DPC, dodecylphosphocholine-d_{38}; E1, first extracellular loop; E2, second extracellular loop; HEPES, *N*-(2-hydroxyethyl)piperazine-*N*′-2-ethanesulfonic acid; kDa, kilodalton(s); M174A/M181A, mutant NK-1 receptor with Met174 and Met181 substituted by Ala; M174A, mutant NK-1 receptor with Met174 substituted by Ala; M181A, mutant NK-1 receptor with Met181 substituted by Ala; MALDI, matrix-assisted laser desorption ionization; NK-1, neurokinin-1 receptor (also substance P receptor); SDS−PAGE, sodium dodecyl sulfate−polyacrylamide gel electrophoresis; SP, substance P; TFA, trifluoroacetic acid; TM, transmembrane; UV, ultraviolet.

in a Centricon SR3 (Amicon, Beverly, MA) which removed excess SDS before V8 treatment. The tryptic receptor fragment was then treated with 10 μg of V8/100 μL incubation volume at room temperature, overnight.

Cyanogen bromide cleavage of photolabeled NK-1 receptors was performed as previously described (*4*). Briefly, membrane preparations of photolabeled NK-1 receptors were adsorbed onto C-18-derivatized silica gel (EM-Science) at 1 g of gel/100 mg of membrane protein and washed with 100% acetonitrile followed by 0.1% trifluoroacetic acid (TFA) in water. The silica gel with the adsorbed photolabeled NK-1 receptor was washed twice with 10 gel volumes of 0.1% TFA and then washed 3 times with 10 gel volumes of acetonitrile/TFA/water (70:0.1:29.9, v/v/v) to remove any noncovalently bound photoligand. The silica gel was equilibrated by washing twice with 10 gel volumes of 0.1 M HCl followed by incubation with or without 50 mg/mL cyanogen bromide (CNBr). After overnight incubation with constant agitation at room temperature in the dark, the silica gel was washed twice with 10 gel volumes of 0.1% TFA to remove the CNBr. CNBr-generated fragments were eluted from the silica gel with acetonitrile/TFA/water (70:0.1:29.9, v/v/v). Radioactivity in the eluates and on the silica gel was measured by γ-spectrometry.

SDS−Polyacrylamide Gel Electrophoresis (PAGE) and Autoradiography. Photoaffinity-labeled receptor membranes and labeled receptor fragments were solubilized in sample buffer (0.125 M Tris, pH 6.8, 2% SDS, 10% glycerol, and 0.01% bromphenol blue) and subjected to SDS−PAGE as described by Laemmli (*12*) and/or the modified Tricine gel system of Schagger and von Jagow (*13*). After electrophoresis, the gels were dried and exposed to X-ray film (XAR 5, Kodak) and developed by a Kodak M35A X-OMAT Processor. Molecular weight markers (Bio-Rad) and prestained Rainbow molecular weight markers (Amersham) were used to assess the molecular weight of the resolved proteins or peptides.

A second SDS−PAGE gel was used to further characterize the previously resolved limit fragments after they were cut from a dried gel, partially rehydrated in sample buffer with 30 mM D,L-dithiothreitol, and incubated for 1 h in a lane of a second gel to allow for the reduction of any disulfide bonds present. The samples were then subjected to SDS−PAGE and autoradiography as described above.

Peptide Synthesis. A fragment of the NK-1 receptor (Ac-FPQGYYSTTETMPSRVVCMIEWPEHPNRTYEKAYHI-NH_2), corresponding to the second extracellular loop (residues 162−198), plus the initial portions of the adjoining transmembrane segments to anchor the peptide in a lipid bilayer, was synthesized by solid-phase methodology at the Protein Chemistry Facility of Tufts University (Boston, MA) using Fmoc chemistry and an Applied Biosystems peptide synthesizer. The purity was established by analytical high-performance liquid chromatography and the structural integrity by mass spectrometry and NMR.

Nuclear Magnetic Resonance. The E2 loop NK-1 receptor peptide (residues 162−198) was examined in aqueous solution (ca. 1.9 mM, 9:1 $H_2O/^2H_2O$, pH 5 not corrected for deuterium), in the presence of 180 mM dodecylphosphocholine-d_{38} [DPC; CIL (Cambridge Isotope Labs), Cambridge, MA]. All of the experiments were recorded on a Bruker DRX 600 MHz spectrometer at temperatures varying between 300 and 318 K. Data processing utilized XWIN NMR, NMRPipe (*14*), or *Felix* (MSI). Chemical shifts were referenced to the signal of tetramethylsilane (0.0 ppm).

The amino acid spin systems were identified from DQF-COSY (*15*) and TOCSY (*16*, *17*) spectra. NOESY (*18*, *19*) experiments with mixing times of 80−350 ms were employed for the sequential assignment. The TOCSY utilized a MLEV-17 sequence to realize mixing times of 35−65 ms with a spin-lock field of 10 000 Hz. Suppression of the solvent signal was achieved using WATERGATE (*20*). The typical spectral width was 7000 Hz in both dimensions, with 2048 data points in t_2 and 720 data points in t_1 and with 8−64 scans at each increment. Both dimensions were multiplied by Gaussian or shifted squared sine bell apodization functions, prior to Fourier transformation.

Structure Calculation. NOESY spectra acquired at 300, 308, and 318 K with mixing times of 100−150 ms were utilized to measure cross-peak volumes (Felix; Molecular Simulations, Inc., La Jolla, CA). The volumes were converted to distances using the two-spin approximation. The resolved cross-peaks between protons at a fixed distance were utilized as reference (Trp184 hz2−Trp184 hh2, 2.47 Å; Pro175 hδ1−hδ2, 1.78 Å; Pro185 hδ1−hδ2, 1.78 Å) (*21*, *22*). Addition and subtraction of 10% to the calculated distances yielded upper and lower bounds. Pseudoatom corrections were applied to methyl groups and methylene protons with coincident chemical shifts (*21*); the floating chirality approach (*23*) was utilized for nonstereospecifically assigned, resolved methylene protons. A home-written program was utilized to calculate an ensemble of 100 structures fulfilling holonomic (constitutional) and experimental (proton−proton distances) restraints. A two-step procedure utilizing random metrization (*24*) followed by optimization via conjugate gradients and distance-driven dynamics (DDD) produced 82 structures (*25*−*27*). This refinement protocol has been tested for a number of NMR-derived structures of peptides (*26*, *28*, *29*), and provides optimal, unbiased sampling of conformational space compatible with the NMR data. The structure was further refined using molecular dynamics simulations as described previously (*30*).

RESULTS

Photoaffinity Labeling of NK-1 Receptor Mutants. To evaluate the effect of substituting Ala for Met174 and/or Met181 in the NK-1 receptor, peptide agonist binding affinities were determined by equilibrium competition binding assays using ^{125}I-Bolton−Hunter-conjugated substance P [^{125}I(BH)-SP]. SP binding to the single mutant NK-1 receptors, M174A and M181A, displayed modest increases in IC_{50} values compared to the wild-type NK-1 receptor, while the double mutant NK-1 receptor, M174A/M181A, displayed a 10-fold increase (Table 1). Equilibrium competition binding assays were then performed using Bpa^4-SP and Bpa^8-SP as the displacing ligands to evaluate the affinity and thus the usefulness of these photoligands for photoaffinity labeling studies on the mutant NK-1 receptors (Table 1). Similar to the parent peptide, these photoligands bind the single mutant NK-1 receptors with only minor changes in IC_{50} values, while a more significant decrease is observed in the double mutant NK-1 receptor (Table 1).

Since Bpa^4-SP and Bpa^8-SP retain high-affinity binding to the mutant NK-1 receptors, we synthesized radiolabeled

Table 1: ^{125}I(BH)-SP Competition Binding Affinities (IC_{50}) for Wild-Type and Mutant NK-1 Receptors[a]

NK-1 receptor	SP (nM)	Bpa^4-SP (nM)	Bpa^8-SP (nM)
WT	0.67 ± 0.38	3.17 ± 1.06	0.77 ± 0.12
M174A	1.43 ± 0.38	6.90 ± 2.95	0.39 ± 0.11
M181A	1.47 ± 0.55	12.50 ± 6.54	0.82 ± 0.16
M174A/M181A	7.53 ± 2.69	63.60 ± 25.44	3.10 ± 0.69

[a] CHO cells expressing wild-type, M174A, M181A, or M174A/M181A NK-1 receptors were incubated for 2 h at 4 °C with ^{125}I(BH)-SP and increasing concentrations of SP, of Bpa^4-SP, or of Bpa^8-SP. The specific binding of ^{125}I(BH)-SP was determined by ultrafiltration assay as described under Experimental Procedures. Specific binding was determined in the presence of excess SP. The average values are calculated from at least three experiments conducted in triplicate.

analogues of the Bpa^4-SP and Bpa^8-SP peptides and evaluated changes in efficiency and/or sites of photoincorporation in the mutant receptors. The efficiency of photoincorporation was calculated by measuring the fraction of the specifically bound photoligand that became covalently attached to the receptor upon UV irradiation. The efficiency of photolabeling of the M181A receptor by ^{125}I(BH)Bpa^8-SP was reduced to 27% (±5) compared to 75% (±3) to the wild-type NK-1 receptor, while photolabeling of M174A (53% ± 8) was also reduced, but as expected by a much lesser extent. Similarly, when ^{125}I(BH)Bpa^4-SP was used to photolabel the M181A NK-1 receptor, the efficiency of photoincorporation was not different from that of the wild-type receptor, 38% (±5) and 37% (±5), respectively. However, ^{125}I(BH)Bpa^4-SP photolabeling of the M174A mutant resulted surprisingly not in a loss of photoincorporation, but in an increase to 55% (±12) photoincorporation. Not surprisingly, removal of both photoattachment sites by mutation (M174A/M181A NK-1 receptor) resulted in very low photoincorporation (less than 5%), for both photoligands, thus preventing further analysis of this mutant receptor.

Receptor Fragmentation Analysis. The sites of covalent attachment of each photoligand to the receptor mutants were assessed using proteolytic digestion with trypsin and fragment resolution on SDS−PAGE. With increasing concentrations of trypsin, the ^{125}I(BH)Bpa^8-SP-photolabeled wild-type NK-1 receptor (WT NK-1) is cleaved to increasingly smaller photolabeled fragments. At a trypsin concentration of 0.1 mg/mL (Figure 1, lane 5), two discrete photolabeled bands of 8 and 5 kDa were observed. These bands represent two distinct limit fragments of trypsin digestion, since incubation with even higher concentrations of trypsin did not convert the 8 kDa fragment to the 5 kDa fragment.

Trypsin digestion of the M181A receptor photolabeled with ^{125}I(BH)Bpa^8-SP yielded only one limit fragment of 5 kDa (Figure 1, lane 13). The absence of the other 8 kDa limit tryptic fragment seen in the wild-type photolabeled receptor correlates well with the reduction in the efficiency of photolabeling of this mutant receptor when compared to the wild-type receptor. Digestion with increasing concentrations of trypsin of the M174A receptor photolabeled with the same ligand, ^{125}I(BH)Bpa^8-SP, yielded progressively smaller photolabeled fragments with a single limit fragment of 8 kDa (Figure 1, lane 9). Thus, the two limit fragments identified after tryptic digestion of the photolabeled wild-type NK-1 receptor are a composite of each of the single limit fragments observed after trypsin digestion of the mutant

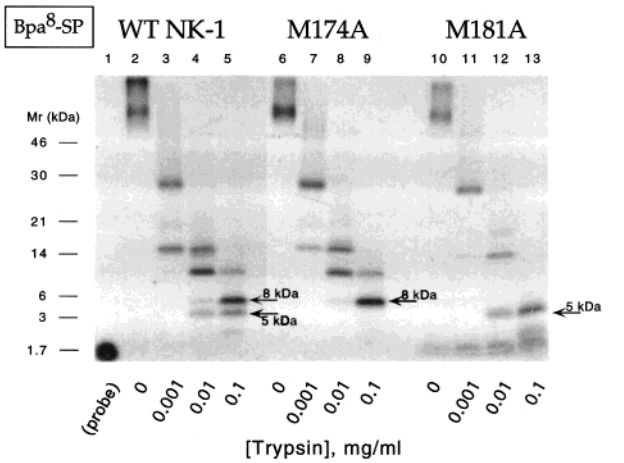

FIGURE 1: SDS−PAGE analysis of trypsinized ^{125}I(BH)Bpa^8-SP-photolabeled wild-type, M174A, or M181A NK-1 receptor. Solubilized ^{125}I(BH)Bpa^8-SP photoaffinity-labeled wild-type (lanes 2−5), M174A (lanes 6−9), or M181A (lanes 10−13) NK-1 receptors were incubated with increasing concentrations of trypsin, as indicated, for 2 h at room temperature with constant agitation. The digested receptors were then subjected to nonreducing SDS−PAGE with Tricine, followed by autoradiography as described under Experimental Procedures. Lane 1 is the photoprobe, ^{125}I(BH)Bpa^8-SP alone. The right, upward slant observed in lane 13 is due to an artifact in running the SDS−PAGE gel.

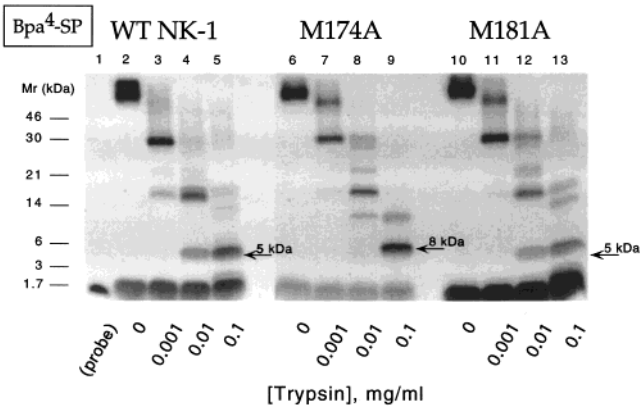

FIGURE 2: SDS−PAGE analysis of trypsinized ^{125}I(BH)Bpa^4-SP-photolabeled wild-type, M174A, or M181A NK-1 receptor. Solubilized ^{125}I(BH)Bpa^4-SP photoaffinity-labeled wild-type (lanes 2−5), M174A (lanes 6−9), or M181A (lanes 10−13) NK-1 receptors were incubated with increasing concentrations of trypsin, as indicated, for 2 h at room temperature with constant agitation. The digested receptors were then subjected to nonreducing SDS−PAGE with Tricine, followed by autoradiography as described under Experimental Procedures. Lane 1 is the photoprobe, ^{125}I(BH)Bpa^4-SP alone. The right, upward slant observed in lane 13 is due to an artifact in running the SDS−PAGE gel.

receptors, M181A and M174A.

Wild-type NK-1 receptors and mutant NK-1 receptors, M174A and M181A, photolabeled with ^{125}I(BH)Bpa^4-SP were also subjected tryptic digest analysis (Figure 2). Tryptic cleavage of the ^{125}I(BH)Bpa^4-SP-photolabeled wild-type NK-1 receptor resulted in a single limit fragment of 5 kDa (Figure 2, lane 5). The limit tryptic fragment of the M181A receptor which photolabels with a similar efficiency as the wild-type receptor also yields a limit fragment of 5 kDa (Figure 2, lane 13). In contrast, the limit tryptic fragment of the M174A mutant receptor, which displays an even higher efficiency of photolabeling than the wild-type receptor, yields a different tryptic digestion pattern and a limit fragment of

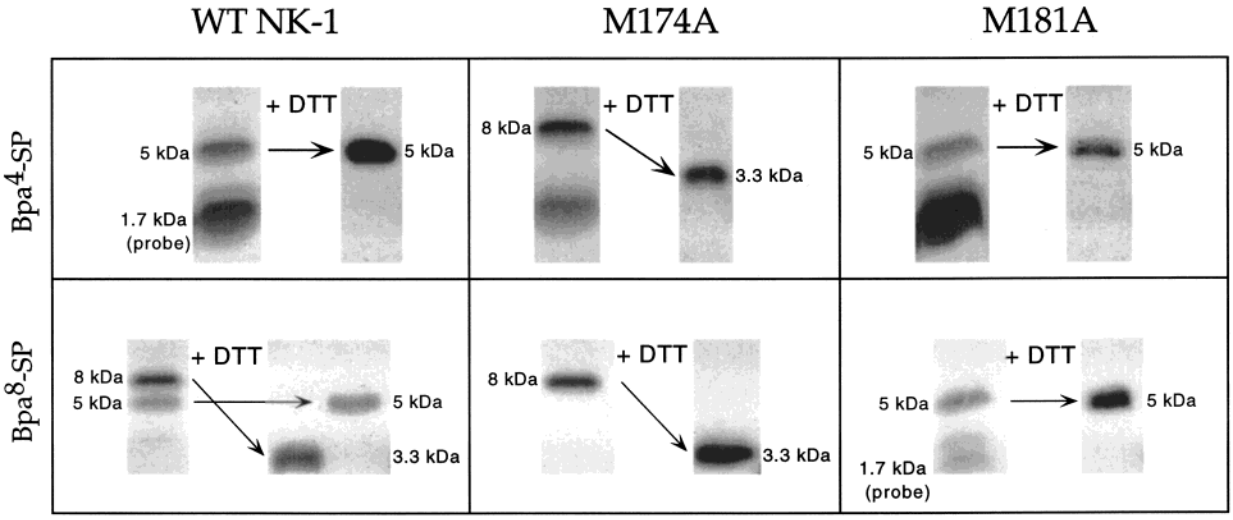

FIGURE 3: SDS−PAGE analysis of ^{125}I(BH)Bpa^4-SP- and ^{125}I(BH)Bpa^8-SP-photolabeled wild-type, M174A, or M181A NK-1 receptor limit tryptic fragments before and after DTT treatment. The indicated wild-type, M174A, and M181A NK-1 receptor tryptic fragments were excised from the dried gel in Figures 1 and 2 (depicted in the left lane of each box above) and allowed to rehydrate in sample buffer with 30 mM DTT while loaded into a second SDS−PAGE gel (right lanes of each box above). The reductive cleavage products were then resolved by SDS−PAGE with Tricine followed by autoradiography as described under Experimental Procedures. The arrows indicate any qualitative shift in mobility in the limit receptor fragment. The difference in apparent band intensity is due to the different exposure times used for autoradiography visualization.

a different size, 8 kDa (Figure 2, lane 9), suggesting a different site of covalent attachment than in the wild-type and M181A mutant receptors.

Previously, we have established that the NK-1 receptor contains a disulfide bond between Cys105 on the E1 loop and Cys180 on the E2 loop that is necessary for high-affinity ligand binding (*31*). Reductive cleavage of photolabeled receptor fragments linked by this disulfide bond has been key to establishing the position of the fragment within the sequence of the receptor. To determine which of the photolabeled limit fragments obtained after tryptic digestion could be reduced in molecular weight by reductive cleavage using D,L-dithiothreitol (DTT), the tryptic fragment bands resolved by SDS−PAGE in Figures 1 and 2 were excised, reduced with DTT, and resolved on a second SDS−PAGE. The molecular mass ~5 kDa limit fragments obtained by trypsin digestion of the ^{125}I(BH)Bpa^4-SP-photolabeled wild-type NK-1 receptors (Figure 2, lane 5) and M181A mutant receptor (Figure 2, lane 13) were not affected by DTT treatment (Figure 3, upper left and right panels). In contrast, the ^{125}I(BH)Bpa^4-SP-photolabeled M174A NK-1 receptor limit fragment of molecular mass ~8 kDa (Figure 2, lane 9) was markedly reduced to molecular mass ~3.3 kDa following DTT treatment (Figure 3, upper middle panel).

Reductive cleavage analysis of the two limit tryptic fragments of the ^{125}I(BH)Bpa^8-SP-photolabeled wild-type NK-1 receptor resulted in the 8 kDa major fragment being reduced to 3.3 kDa, while the 5 kDa minor fragment was unaffected by DTT treatment (Figure 3, lower left panel). The 8 kDa fragment produced by trypsin digestion of the ^{125}I(BH)Bpa^8-SP-photolabeled M174A NK-1 receptor was also reduced to 3.3 kDa with DTT treatment (Figure 3, lower middle panel), while the 5 kDa fragment produced by trypsin digestion of ^{125}I(BH)Bpa^8-SP-photolabeled M181A receptor was unaffected by DTT treatment (Figure 3, lower right panel).

To localize further the photoattachment sites for ^{125}I(BH)-Bpa^4-SP and ^{125}I(BH)Bpa^8-SP on the M174A and M181A NK-1 receptors, the photolabeled receptors were subjected to cyanogen bromide (CNBr) cleavage and the resultant fragments resolved by SDS−PAGE (Figure 4). For the wild-type receptor and each mutant NK-1 receptor, a band centered at less than 2 kDa was observed. This does not correspond to any of the theoretical CNBr-digestion fragments, but rather is similar in size to the photoprobe itself. Nevertheless, this band is not the free ligand since that has been removed from the solid-phase absorbed photolabeled complex prior to treatment with CNBr (*4*). This 2 kDa product, which we have previously characterized by isolation

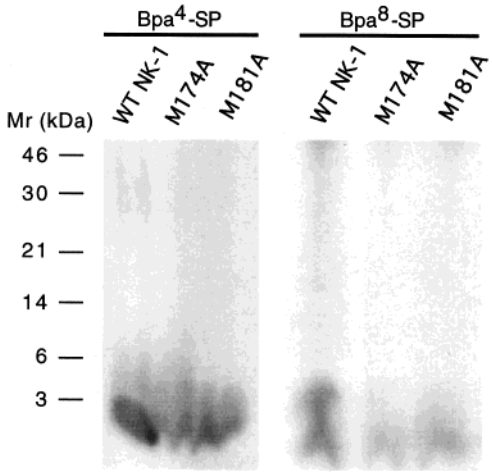

FIGURE 4: SDS−PAGE analysis of CNBr-treated ^{125}I(BH)Bpa^4-SP- or ^{125}I(BH)Bpa^8-SP-photolabeled wild-type, M174A, or M181A NK-1 receptors. ^{125}I(BH)Bpa^4-SP and ^{125}I(BH)Bpa^8-SP photoaffinity-labeled wild-type, M174A, or M181A NK-1 receptors were adsorbed onto C18 silica gel, washed to remove noncovalently attached photoligand, and then treated with 50 mg/mL CNBr overnight at room temperature with constant agitation. Receptor fragments were eluted from the silica gel with 70% ACN in 0.1% TFA. The digested receptors were then subjected to nonreducing SDS−PAGE with Tricine, followed by autoradiography as described under Experimental Procedures. Note: ^{125}I(BH)Bpa^4-SP is labeled Bpa^4-SP, and ^{125}I(BH)Bpa^8-SP is labeled Bpa^8-SP.

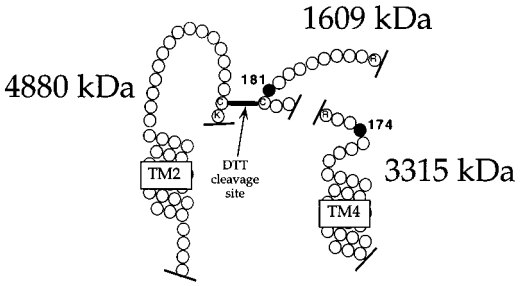

FIGURE 5: Reductive cleavage illustration of tryptic NK-1 receptor limit fragments. NK-1 receptor fragments resulting from trypsin cleavage are represented as chains of circles or residues. The calculated molecular mass of each fragment is indicated next to it. The 4880 kDa fragment (TM2 and the E1 loop) is bound to the 1609 kDa fragment (partial E2 loop) by a disulfide bond between Cys105 and Cys180, resulting in a 6489 kDa limit tryptic fragment. This bond is chemically reduced by DTT treatment, resulting in two receptor fragments of 4880 and 1609 kDa. The 3315 kDa fragment (partial E2 loop/TM4) contains no Cys residues and is thus not affected by DTT treatment. Met174 and Met181 are labeled and represented by closed black circles.

and MALDI mass spectroscopy, is the product that results from CNBr cleavage of a methionine residue when the site of covalent photoattachment is to the CH_3 group of that methionine residue.

Sites of Covalent Attachment. The sites of covalent attachment for ^{125}I(BH)Bpa^4-SP and ^{125}I(BH)Bpa^8-SP to the M174A and M181A mutant NK-1 receptors were determined by comparing the results of the fragmentation analyses of the wild-type and mutant receptors. Of particular diagnostic importance is the disulfide bond between Cys105 in the first extracellular (E1) loop and Cys180 in the E2 loop. As illustrated in Figure 5, reductive cleavage of this disulfide bond in a limit trypsin fragment from a photolabeled NK-1 receptor would result in smaller limit fragments only if photoattachment had occurred to a residue on a proteolytic fragment containing either of these Cys residues (either the TM2/E1 loop fragment of 4880 kDa or the partial E2 loop fragment of 1609 kDa); whereas if photoattachment had occurred to a residue not on a Cys-containing receptor fragment (such as the partial E2 loop/TM4 3315 kDa fragment), no smaller limit fragments would be observed after reductive cleavage. Therefore, we are able to distinguish between labeling of Met174 on the 3315 kDa receptor fragment and Met181 on the 4880 kDa receptor fragment using this analysis.

Photoaffinity labeling of the wild-type NK-1 receptor with ^{125}I(BH)Bpa^8-SP and subsequent tryptic receptor fragmentation analysis revealed two sites of covalent attachment. The primary site (~67% of the observed labeling) is contained within the 8 kDa fragment, which is reduced in molecular mass to 3.3 kDa following DTT treatment. There are only two possible tryptic fragments on the NK-1 receptor that correspond to that molecular mass minus the photoligand (~1.7 kDa): (i) the amino terminus, and (ii) the TM2/E1 covalently bound to part of E2 (Figure 6A). However, due to the heavy glycosylation of the amino terminus, the molecular mass of this fragment would be much greater than 8 kDa. Additionally, the latter candidate is in agreement with the results of DTT treatment observed in Figure 3; thus, the 3.3 kDa fragment following reductive cleavage limits the covalent attachment site to residues 178−190. In view of

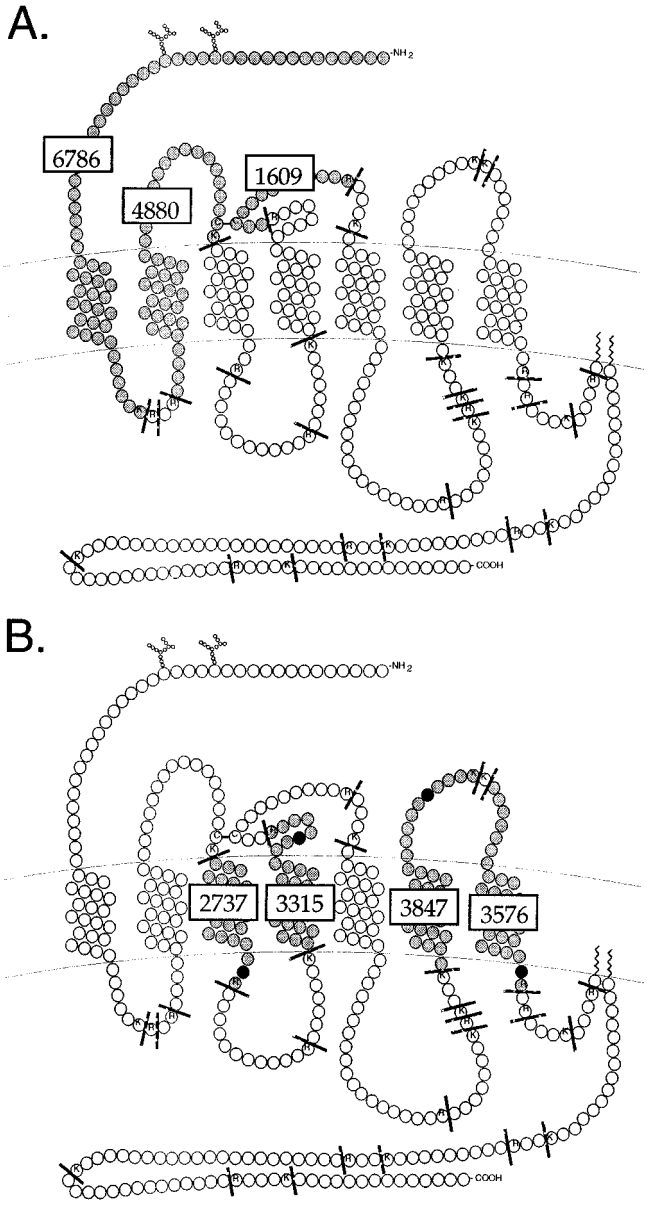

FIGURE 6: Candidate photolabeled tryptic receptor fragments. Serpentine diagram of the NK-1 receptor with seven transmembrane domains connected by intra- and extracellular loops and termini. Panel A illustrates two candidate 8 kDa photolabeled limit fragments in gray: a 6786 kDa fragment and a 6489 kDa fragment comprising the disulfide bound fragments of 4880 and 1609 kDa. Note: to correlate these molecular masses to the photolabeled fragments, add the molecular mass of the photoligand, 1.7 kDa. Panel B illustrates four candidate 5 kDa limit fragments in gray. V8 protease subcleavage sites are indicated as closed black circles.

the CNBr cleavage results, and that the only methionine residue within this sequence is Met181, it can be concluded that this residue is the site of covalent attachment, in agreement with our previous results (*4, 31*).

Interestingly, the secondary site of covalent attachment of ^{125}I(BH)Bpa^8-SP on the wild-type NK-1 receptor (~33% of the observed labeling) is to a tryptic receptor fragment apparently equivalent to that photolabeled on the M181A NK-1 receptor mutant where the primary site of covalent attachment has been mutated. These 5 kDa limit fragments are not reduced in molecular mass upon DTT treatment. Therefore, four possible tryptic receptor fragments correspond to this molecular mass (Figure 6B). The candidate

fragments from TM6 and TM7 are eliminated due to the size of the intermediate fragments and based on previous data (*31*). Therefore, the TM3 and TM4 fragments are the remaining possible sites of covalent attachment. Since the 5 kDa fragment is reduced in molecular mass to ~3 kDa by V8 protease subcleavage (data not shown), the fragment covalently attached must be the TM4/E2 fragment since it contains a V8 cleavage site that would result in a 3 kDa product. Thus, the subcleaved fragment must correspond to residues 170−177. Cyanogen bromide treatment of both wild-type and M181A mutant NK-1 receptors photolabeled with ^{125}I(BH)Bpa^{8}-SP also indicated that photoattachment is to a methionine residue. Thus, Met174 is the covalent attachment site on the M181A mutant NK-1 receptor and is the secondary site of covalent attachment on the wild-type NK-1 receptor.

Likewise, the tryptic cleavage of ^{125}I(BH)Bpa^{4}-SP-photolabeled wild-type NK-1 receptor generated a 5 kDa limit fragment which was not decreased in size upon DTT treatment and therefore does not contain Cys105 or Cys180. The labeled receptor fragment must therefore correspond to residues 142−177 based on its size and the absence of either cysteine residue. Since CNBr treatment of this photolabeled receptor indicates that the site of attachment is to a methionine residue within that sequence, Met174 is confirmed to be the site of covalent attachment of ^{125}I(BH)-Bpa^{4}-SP to the wild-type NK-1 receptor as previously reported (*5*). Based on similar observations, the same conclusion is made for the site of covalent attachment of ^{125}I(BH)Bpa^{4}-SP to the M181A mutant NK-1 receptor as the wild-type receptor: Met174. However, when Met174 is replaced by Ala, the site of covalent attachment is not to the substituted residue, nor is it to a site on the Met174 containing tryptic fragment (residues 142−177). Analysis of the 8 kDa limit tryptic fragment generated from the M174A mutant NK-1 receptor photolabeled with ^{125}I(BH)Bpa^{4}-SP indicates that it contains either Cys105 or Cys180 since it is reduced to a molecular mass of 3.3 kDa following DTT treatment. This fragment must then correspond to residues 178−190 based on the sizes of the limit fragments before and after reduction; and since CNBr cleavage of this ^{125}I(BH)Bpa^{4}-SP-photolabeled mutant NK-1 receptor indicates covalent attachment to a methionine residue, Met181 is concluded to be the site of covalent attachment.

Structural Preferences of the E2 Loop of the NK1 Receptor. The combination of phototaffinity labeling and point mutational analysis has thus provided a direct means to analyze the proximity of the photoligand to specific residues in the receptor structure. Specifically, both Met174 and Met181 on the NK-1 receptor have been previously identified as photoattachment sites of benzophenone containing derivatives of SP. Here, the relationship between these residues has been investigated by taking into account both the photochemistry of the benzophenone moiety and the dimensions of the substituted residues in the mutant NK-1 receptors. We then sought to examine the structural relationship between these sites of covalent attachment using spectroscopic methodologies.

NMR analyses were performed on a synthetic peptide corresponding to this domain, residues 162−198, which contains the entire putative E2 loop of the NK-1 receptor, flanked by several residues of the fourth and fifth transmembrane helices. These residues were included to anchor and orient the receptor fragment into micelles, as has been successfully used in fragment studies of the parathyroid hormone receptor (*7, 32*−*34*). The termini of the peptide were blocked as acetyl and amide derivatives, respectively, to remove the charges of the termini. The DPC micelles provide a charged zwitterionic interface and a hydrophobic core that mimic the molecular environment of biological membranes while allowing high-resolution NMR studies. The DPC concentration was chosen as to provide more than one micelle per each peptide molecule (*35*−*37*).

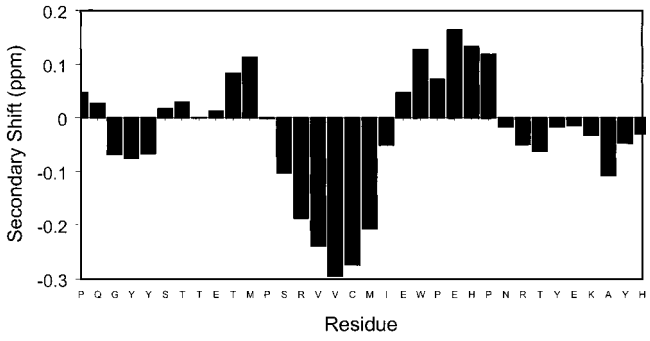

FIGURE 7: Secondary shifts of Hα of NK-1 receptor peptide (residues 162−198) in aqueous solution (pH 5.0, 308 K) in the presence of DPC micelles.

The observed secondary shifts for the α protons provide a qualitative indication of secondary structure and its location in the peptide sequence. The secondary shifts were calculated by subtracting the chemical shifts for unstructured peptides (*21*) from the experimentally measured chemical shifts, and averaging the values over succeeding triplets of amino acids (*38*). The negative values observed for Ser176−Ile182 (Figure 7) are consistent with an α-helical structure (*39*), while smaller deviation at the N- and the C-terminus may indicate scarcely populated helices. Inversions at the level of Pro175 and Pro188 may indicate turns (*39*). [See Supporting Information for a table of the NOEs used in the structure determination.]

A series of correlations of type H^{N}_{i} to H^{N}_{i+1} or H^{N}_{i+2}, and H^{α}_{i} to H^{N}_{i+3} or H^{N}_{i+4} confirm the presence of a well-defined α-helix between residues Pro175 and Glu183. The correlations Pro163 Hα−Tyr166 HN/Hδ,γ; Glu165 HN−Tyr167 HN; Ala195 $CH_3\beta$−Ile198 HN; Ala195 $CH_3\beta$−Ile198 NH_2; Tyr192 Hγ−Ala195 $CH_3\beta$; and Tyr196 HN−Ile198 HN indicate the tendency of the sequences putatively corresponding to the top of TM4 and TM5 to fold into α-helices. The content of α-helix determined by NMR is in agreement with the estimated percentage of helix obtained from CD measurements (data not shown). In addition, a turn following the central helix is identified by an NOE of type H^{α}_{i} to H^{N}_{i+2} between Pro185 and His187 and side-chain-to-side-chain NOEs of residues Glu183−His187. A possible subsequent turn is suggested by NOEs His187 Hα−Asn189 HN and Glu186 Hα−Asn189 HN.

A total of 82 structures were obtained from the DG calculations, with no NOE violation larger than 0.2 Å. The structures converge to a fairly regular α-helical segment encompassing residues 176−182 (average pairwise RMSD: 0.92 Å) with one additional irregular loop toward the N-terminus (to Met174). The dihedral angle order parameters for ϕ and ψ (data not shown) indicate a high degree of order

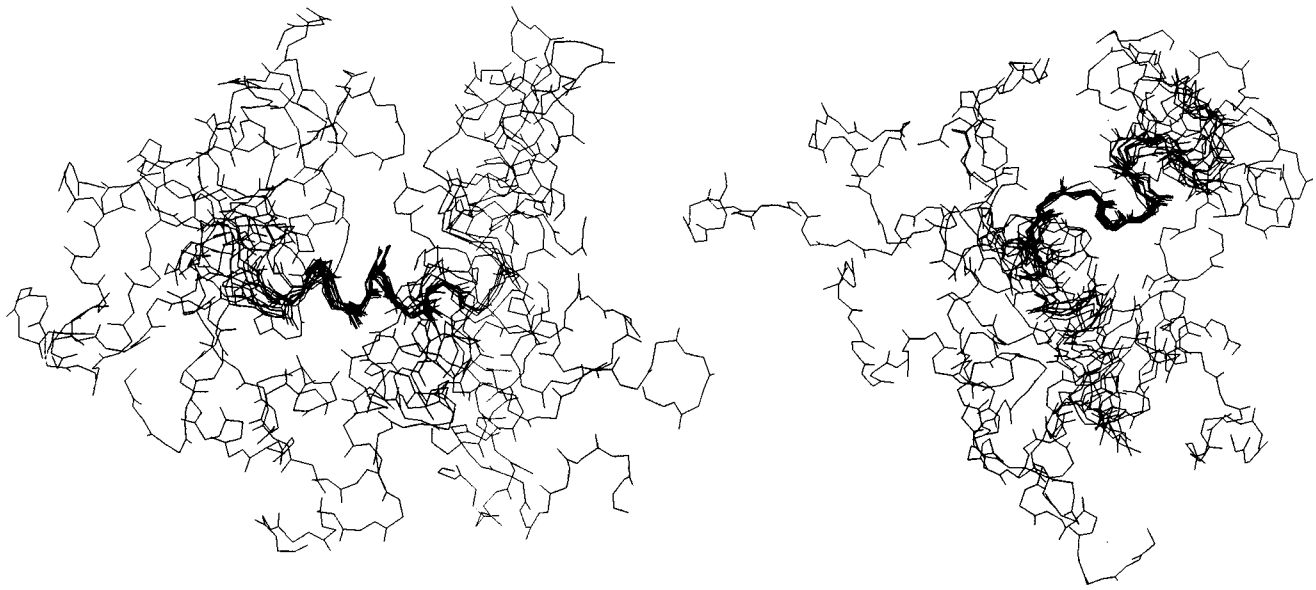

FIGURE 8: NMR-based structure of the NK-1 receptor E2 loop. Superposition of 30 structures of the NK-1 receptor peptide (residues 162−198) obtained from DG calculations (see text for details). The heavy backbone atoms of residues 175−183, the central α-helix (left), and 185−189 (right) were used in the superposition. Although these structural elements are well determined, the regions between them produce the illustrated dispersion.

also in the region 184−188, that appears to be characterized by two sequential irregular turns. A flexible point at residue 181 separates the two regions of order.

The distance separating the N- from the C-terminus is highly variable, as expected for a linear peptide, encompassing distances between 10 and 44 Å (mean: 27 Å ± 10). The theoretical distance between the two TM helices [approximately 13 Å based on the rhodopsin model (*40*)] is also populated and compatible with all experimental data. Thirty structures from the DG calculations are represented in Figure 8. The structures have been superimposed in the region of the central helix (left panel) and in the turn region (right panel). The central α-helix of the E2 loop limits the range of distances between Met174 and Met181. The distance between these residues (using Cα atoms) over the resulting 82 DG structures is 11.3 ± 1.0 Å.

DISCUSSION

Previous results have established that the primary site of covalent attachment of ^{125}I(BH)Bpa^{8}-SP is Met181 on the wild-type NK-1 receptor (*4*) and that the primary site of covalent attachment of ^{125}I(BH)Bpa^{4}-SP on the wild-type NK-1 receptor is Met174 (*5*, *41*). These results directed the construction of mutant receptors in which each of these two methionine residues was substituted individually by alanine. In addition, a doubly mutated receptor in which both Met181 and Met174 were substituted by alanine was also constructed.

SP binds to the mutant NK-1 receptors, M174A and M181A, with modest decreases in agonist affinity, whereas SP binding to the M174A/M181A mutant NK-1 receptor occurs with a more marked decrease in affinity. This small loss in affinity when a single contact site is removed has been found previously for other peptide ligands that form multiple contacts with their receptors (*42*). Both single point mutant NK-1 receptors are functional in an intracellular calcium flux assay using a fluorescent calcium indicator, Fura-2/Am. The maximal responses observed were equal to that of the wild-type NK-1 receptor (unpublished results). The mutant NK-1 receptors are thus capable of forming a specific conformation that binds SP with high affinity, initiating receptor-mediated cellular signal transduction.

When we removed the primary site of photoincorporation for ^{125}I(BH)Bpa^{8}-SP, Met181, from the NK-1 receptor, we observed a marked decrease in photolabeling efficiency, and the residual photolabeling was to Met174, a secondary site of photolabeling on the NK-1 receptor. In contrast, ^{125}I(BH)-Bpa^{4}-SP photolabels Met174 in the wild-type NK-1 receptor exclusively; thus, position 4 in the SP peptide is in close spatial proximity to Met174. Surprisingly, when this site of photoinsertion was eliminated by replacement by alanine, photoincorporation now occurred at Met181. Additionally, when both methionine residues are replaced, essentially no photolabeling was observed. These results validate our previous findings and extend our working model of the SP/NK-1 receptor complex by showing that position 4 of SP is spatially proximal to Met174, and that position 8 of SP is closest to Met181, while also being in the general vicinity of Met174. Moreover, these two key methionine residues on the E2 loop of the NK-1 receptor must also be in close proximity to one another.

Information on the relative arrangement of the seven transmembrane helices in G protein-coupled receptors (GPCRs) is based on previous detailed structural studies of rhodopsin (*43*), but little is known about the structures of the intra- and extracellular termini and loops of GPCRs. The determination of these structural elements is essential for understanding the biomolecular interactions between agonists and heterotrimeric G proteins with their specific receptors (*32*, *34*, *44*−*47*).

To provide structural information concerning the E2 loop and in particular the structural relationship between Met174 and Met181 on the NK-1 receptor, a spectroscopic investigation was undertaken. Since NMR of entire transmembrane receptors cannot be examined by conventional methods, we

studied the synthetic peptide corresponding to the entire E2 loop of the rat NK-1 receptor flanked by several residues of the TM4 and TM5 segments (residues 162−198). This peptide readily associated with the DPC micelles, which provided an NMR-compatible solvent system which mimicked the interface between the membrane and extracellular milieu. The current findings that a central portion, residues 175−183, folds into an α-helical structure provides a conformational constraint between Met174 and Met181 of 11.3 Å ± 1. It is important to note, that assuming a typical α-helix, Met174 and Met181 would be on the same helical face (700° about the helical wheel, assuming 100° per residue), thus allowing these residues access to positions 4 and 8 of the agonist SP when bound to the NK-1 receptor, consistent with the results obtained by photolabeling of the receptor mutants. Structural studies of the SP peptide (RPKPQQFFGLM-NH_2) have shown a preference for a helix-like arrangement of the central portion of the ligand, beginning at residue 4, positioning the side chains of 4 and 8 in the same direction (*48*−*51*). Since the structural features of the ligand and receptor fragment have been determined in isolation, there could be conformational changes to these structures upon ligand binding; however, the possibility of a helix−helix interaction between the central portion of the ligand and the E2 loop of the NK1 receptor is very intriguing. Such an interaction is consistent with the ligand/receptor contact points directly determined by photoaffinity labeling and the structural preferences of the ligand and of the NK-1 receptor E2 loop. At this stage, however, one must consider this as only a working model; additional photoaffinity labeling and structural studies are certainly required to test, refine, and expand this evolving, experimentally based model of the SP/NK1 receptor complex. This model will help evaluate the biomolecular interface between SP and the NK-1 receptor which is necessary for understanding the molecular basis of peptide recognition and receptor activation and may also provide a framework for structure-based design of novel therapeutic agents.

SUPPORTING INFORMATION AVAILABLE

Four pages listing data for structurally informative NOEs (4 pages). This material is available free of charge via the Internet at http://pubs.acs.org.

REFERENCES

1. Otsuka, M., and Yoshioka, K. (1993) *Physiol. Rev. 73*, 229−308.
2. Kauer, J. C., Erickson-Viitanen, S., Wolfe, H. R., Jr., and DeGrado, W. F. (1986) *J. Biol. Chem. 261*, 10695−10700.
3. Boyd, N. D., White, C. F., Cerpa, R., Kaiser, E. T., and Leeman, S. E. (1991) *Biochemistry 30*, 336−342.
4. Kage, R., Leeman, S. E., Krause, J. E., Costello, C. E., and Boyd, N. D. (1996) *J. Biol. Chem. 271*, 25797−25800.
5. Li, H., Macdonald, D., Hronowski, X., Costello, C. E., Leeman, S. E., and Boyd, N. D. (2001) *J. Biol. Chem*. (in press) (published online Dec 14, 2000).
6. Greenberg, Z., Bisello, A., Mierke, D. F., Rosenblatt, M., and Chorev, M. (2000) *Biochemistry 39*, 8142−8152.
7. Piserchio, A., Bisello, A., Rosenblatt, M., Chorev, M., and Mierke, D. F. (2000) *Biochemistry 39*, 8153−8160.
8. Sachais, B. S., Snider, R. M., Lowe, J. A., and Krause, J. E. (1993) *J. Biol. Chem. 268*, 2319−2323.
9. Sanger, F., Nicklen, S., and Coulson, A. (1977) *Proc. Natl. Acad. Sci. U.S.A. 74*, 5463−5467.
10. Sachais, B. S., and Krause, J. E. (1994) *Mol. Pharmacol. 46*, 122−128.
11. Li, H., Leeman, S. E., Slack, B. E., Hauser, G., Saltsman, W. S., Krause, J. E., Blusztajn, J. K., and Boyd, N. D. (1997) *Proc. Natl. Acad. Sci. U.S.A. 94*, 9475−9480.
12. Laemmli, U. K. (1970) *Nature (London) 227*, 680−685.
13. Schagger, H., and Jagow, G. v. (1987) *Anal. Biochem. 166*, 368−379.
14. Delaglio, F., Grzesiek, S., Vuister, G. W., Zhu, G., Pfeifer, J., and Bax, A. (1995) *J. Biomol. NMR 6*, 277−293.
15. Rance, M., Sørensen, O. W., Bodenhausen, G., Wagner, G., Ernst, R. R., and Wüthrich, K. (1983) *Biochem. Biophys. Res. Commun. 117*, 458−479.
16. Braunschweiler, L., and Ernst, R. R. (1983) *J. Magn. Reson. 53*, 521−528.
17. Bax, A., and Davis, D. G. (1985) *J. Magn. Reson. 65*, 355−360.
18. Jeener, J., Meier, B. H., Bachmann, P., and Ernst, R. R. (1979) *J. Chem. Phys. 71*, 4546−4553.
19. Macura, S., Huang, Y., Suter, D., and Ernst, R. R. (1981) *J. Magn. Reson. 43*, 259−281.
20. Piotto, M., Saudek, V., and Sklenar, V. (1992) *J. Biomol. NMR 2*, 661−665.
21. Wüthrich, K. (1986) *NMR of Proteins and Nucleic Acids*, Wiley, New York.
22. Cavanagh, J., Fairbrother, W. J., Palmer, A. G., and Skelton, N. J. (1996) *Protein NMR Spectroscopy, Principle and Practice*, Academic Press, New York.
23. Weber, P. L., Morrison, R., and Hare, D. (1988) *J. Mol. Biol. 204*, 483−487.
24. Havel, T. F. (1991) *Prog. Biophys. Mol. Biol. 56*, 43−78.
25. Kaptein, R., Boelens, R., Scheek, R. M., and van Gunsteren, W. F. (1988) *Biochemistry 27*, 5389−5395.
26. Mierke, D. F., Kurz, M., and Kessler, H. (1994) *J. Am. Chem. Soc. 116*, 1042−1049.
27. Jahnke, W., Mierke, D. F., Beress, L., and Kessler, H. (1994) *J. Mol. Biol. 240*, 445−458.
28. Mierke, D. F., Geyer, A., and Kessler, H. (1994) *Int. J. Pept. Protein Res. 44*, 325−331.
29. Pellegrini, M., Gobbo, M., Rocchi, R., Peggion, E., Mammi, S., and Mierke, D. F. (1996) *Biopolymers 40*, 561−569.
30. Pellegrini, M., Royo, M., Rosenblatt, M., Chorev, M., and Mierke, D. F. (1998) *J. Biol. Chem. 273*, 10420−10427.
31. Boyd, N. D., Kage, R., Dumas, J. J., Krause, J. E., and Leeman, S. E. (1996) *Proc. Natl. Acad. Sci. U.S.A. 93*, 433−437.
32. Pellegrini, M., Royo, M., Chorev, M., and Mierke, D. F. (1996) *J. Pept. Sci. 40*, 653−666.
33. Pellegrini, M., Bisello, A., Rosenblatt, M., Chorev, M., and Mierke, D. F. (1998) *Biochemistry 37*, 12737−12743.
34. Mierke, D. F., Royo, M., Pellegrini, M., Sun, H., and Chorev, M. (1996) *J. Am. Chem. Soc. 118*, 8998−9004.
35. McDonnel, P. A., and Opella, S. J. (1993) *J. Magn. Reson. B 102*, 120−125.
36. Kallick, D. A., Tessmer, M. R., Watts, C. R., and Li, C. (1995) *J. Magn. Reson. B 109*, 60−65.
37. Opella, S. J., Marassi, F. M., Gesell, J. J., Valente, A. P., Kim, Y., Oblatt-Montal, M., and Montal, M. (1999) *Nat. Struct. Biol. 6*, 374−379.
38. Pastore, A., and Saudek, V. (1990) *J. Magn. Reson. 90*, 165−176.
39. Wishart, D. S., Sykes, B. D., and Richards, F. M. (1992) *Biochemistry 31*, 1647−1651.
40. Baldwin, J. M., Schertler, G. F., and Unger, V. M. (1997) *J. Mol. Biol. 272*, 144−164.
41. Li, H. (1997) Doctoral Dissertation, Boston University School of Medicine, Boston, MA.
42. Clackson, T., and Wells, J. A. (1995) *Science 267*, 383−386.
43. Palczewski, K., Kumasaka, T., Hori, T., Behnke, C. A., Motoshima, H., Fox, B. A., Le Trong, I., Teller, D. C., Okada, T., Stenkamp, R. E., Yamamoto, M., and Miyano, M. (2000) *Science 289*, 739−745.
44. Yeagle, P. L., Alderfer, J. L., and Albert, A. D. (1997) *Biochemistry 36*, 9649−9654.

45. Pervushin, K. V., Orekhov, V., Popov, A. I., Musina, L., and Arseniev, A. S. (1994) *Eur. J. Biochem. 219*, 571−583.
46. Pashkov, V. S., Balashova, T. A., Zhemaeva, L. V., Sikilinda, N. N., Kutuzov, M. A., Abdulaev, N. G., and Arseniev, A. S. (1996) *FEBS Lett. 381*, 119−122.
47. Pellegrini, M., Bisello, A., Rosenblatt, M., Chorev, M., and Mierke, D. F. (1998) *Biochemistry 37*, 12737−12743.
48. Auge, S., Bersch, B., Tropis, M., and Milon, A. (2000) *Biopolymers 54*, 297−306.
49. Whitehead, T. L., McNair, S. D., Hadden, C. E., Young, J. K., and Hicks, R. P. (1998) *J. Med. Chem. 41*, 1497−1506.
50. Seelig, A., Alt, T., Lotz, S., and Holzemann, G. (1996) *Biochemistry 35*, 4365−4374.
51. Woolley, G. A., and Deber, C. M. (1987) *Biopolymers 26*, S109−S121.

BI001880X